Christian Renner and Volker Turau. State-of-Charge Assessment for Supercap-Powered Sensor Nodes: Keep it Simple Stupid! In Proceedings of the International Workshop on Algorithms and Concepts for Networked Sensing Systems Powered by Energy Harvesters, EnHaNSS '12, Antwerp, Belgium, June 2012.

State-of-Charge Assessment for Supercap-Powered Sensor Nodes: Keep it Simple Stupid!

Christian Renner and Volker Turau, Institute of Telematics, Hamburg University of Technology, Germany

***Abstract*—Electric double-layer capacitors, also known as supercaps, have several advantages over traditional energy buffers: They do not require complex charging circuits, offer virtually unlimited charge-discharge cycles, and generally enable easy state-of-charge assessment. A closer look yet reveals that leakage and internal reorganization effects hamper state-of-charge assessment by means of terminal voltage, particularly after a charging cycle. Sophisticated models capture this effect at the cost of an increased calculation and parameter-estimation complexity. As this is hardly feasible on low-power, low-resource sensor nodes, we evaluate the performance of simple models on a real energy-harvesting sensor node platform. We show that model errors are as low as 1-2% on average and never exceed 5% in our experiments, supporting that there is no need to employ more complex models on common sensor node platforms, equipped with unreliable ADC readings and uncertain consumption due to hardware variation in the same order of magnitude.**

***Index Terms*—Energy harvesting, Energy measurement, Supercapacitors, Wireless Sensor Networks**

I. Introduction

Energy-harvesting sensor nodes [1]–[3] have the potential and aspiration to extinct the burden of battery replacement in many scenarios. Various harvesting sources can be used, e.g., sunlight, radio frequency, vibration, or temperature differences. Particularly sunlight is promising, since it produces a sufficient amount of energy to supply sensor nodes drawing several µA in sleep state and some mA in full-operation mode.

Unfortunately, the amount of harvested energy is neither constant nor continuous. In case of solar harvesting, energy can exclusively be scavenged during daytime, and its extent depends on weather conditions, time of the year, and placement. As a result, energy must be buffered, so that nodes do neither suffer from temporal energy shortage nor is their operation restricted to periods of incoming energy.

Thorough state-of-charge assessment of the energy buffer is required to achieve perpetual and maximum harvest utility operation via load adaptation algorithms [4], [5]. Although various energy buffer technologies are available on the market, most solutions do not comply with this requirement. State-of-charge assessment depends on the charging history, discharging rate, and temperature. Many buffer technologies have additional drawbacks, such as large size, high costs, and the need for complex charging circuits.

This research has been partially funded by the German Research Foundation under contract number TU 221/4-1

Recently, a promising energy storage technology has become available and affordable: electric double-layer capacitors, also called supercaps. They fill the gap between capacitors and rechargeable batteries and can store enough energy to keep sensor nodes operational for multiple days without recharging. Their main advantage over rechargeable batteries is the high number of possible charge-discharge cycles and that they can be charged and discharged at almost any temperature. While a lifetime of 2-3 years can be expected for lithium-ion polymers, supercaps can last for 10 years or even more. Moreover, supercaps do not need a complex charging circuit.

Reading the manufacturers' data sheets [6], it is tempting to assume that state-of-charge determination can be broken down to measuring a supercap's voltage. Recent research activities in this field have yet reported that this is not entirely true [7], [8]: Leakage and internal reorganization effects affect the voltage. Modeling these effects is yet complex and involves calibration of several parameters per supercap [8].

Using complex models with high calibration effort is not an option for algorithms running on sensor nodes. They have low computation power only, so that wasting energy due to complex calculations and prolonged calibration of a highly parametrized model is not desirable. Moreover, the following reasons suggest that a too complex model overstates the case. Firstly, the presence of hardware variation affects sensor precision and current consumption. Secondly, unknowns—such as the future harvest—impact the available energy resources. Thirdly, unaccounted or unidentified parameters, such as temperature or hardware aging, may render models overfitted.

In this paper, we hence analyze the accuracy of simple charging- and discharging models that can be efficiently run on low-power, low-resource devices. For this purpose, we present an energy-harvesting prototype power supply for sensor nodes that enables practical experiments to obtain real-world evaluation results. We derive models for lifetime prediction and remaining charging time. Running several charging-discharging-cycles at common sensor node duty cycles using a small-sized solar cell, we evaluate the accuracy of our models under realistic conditions. We finally comment on possible methods for quick and reliable self-calibration of a supercap's capacity.

II. Related Work

Various self-sustaining power supplies for wireless sensor nodes exist. Prometheus [1] is based on a two-stage energy storage system consisting of a supercap as the primary energy source and a rechargeable Li^+ battery. The supercap conserves

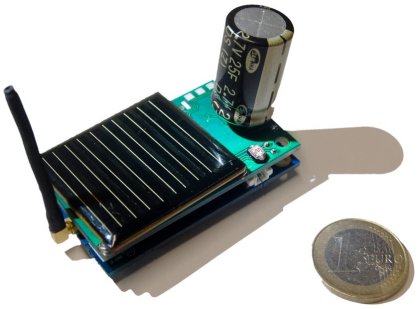

Fig. 1. Energy harvester hardware with solar cell and 25 F supercap

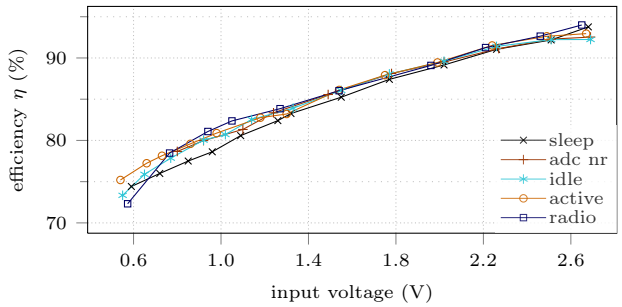

Fig. 2. Measured unbiased regulator efficiency for relevant input voltages and typical Iris node loads

the battery by limiting its charging and discharging cycles. In the corresponding paper, charging and discharging behavior of the circuit and supercap are examined. The authors take a first step into the direction of energy-aware scheduling by adapting the duty cycle to the current supercap voltage. Prometheus has been successfully deployed in the Trio testbed [9]. The Everlast platform stores energy harvested by a solar cell in a supercap solely [2]. Maximum power point tracking (MPPT) is employed in order to increase the efficiency of the solar cell, i.e., the electrical power produced by the cell is maximized. The authors claim that their platform can operate for up to 20 years while preserving high data rates.

Detailed studies about the charging and discharging behavior of supercaps exist. Barrade and Rufer discuss energy and power density of supercaps [10] and derive analytical models. Previous work of the authors of this paper introduces a model for accounting supercap leakage [7]. Weddel et al. substantiate that supercaps do not follow an ideal capacitor's model [8]. They propose a multi-layer cascade-circuit model of resistors and ideal capacitors and discuss its accuracy. The authors of [11] use a piece-wise approximation to model and capture supercap leakage. Both works are highly relevant for system design and supercap simulation, yet online parameter estimation appears to be complex and unreliable for sensor nodes. The latter assumption is due to low ADC precision in most cheap sensor node platforms.

III. Energy-Harvesting Power Supply

We built a customized energy-harvesting power supply (*harvester*) for the Iris sensor node. Figure 1 portrays the harvester mounted on an Iris node with removed battery pack.

A. Hardware Description

1) Harvesting Source: A solar cell with a maximum current of 35 mA and a size of 39×39 mm^2 serves as harvesting source. We chose a direct charging circuit instead of a maximum power-point tracker as in [2]. The advantages are a simple, low-cost circuit and a charging current only depending on lighting conditions. The main disadvantage is that the harvested energy depends on the supercap voltage. The harvester provides a sensor for measuring the current produced by the solar cell. This is achieved by measuring and amplifying the voltage induced by the solar current across a 1 Ω shunt resistor (1% precision).

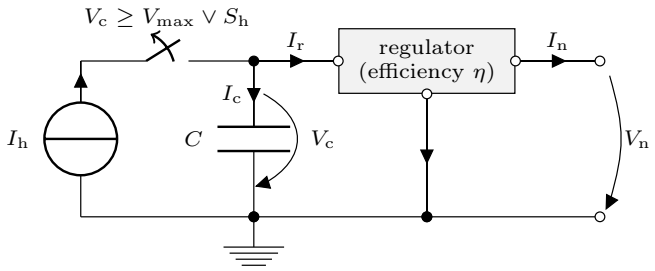

Fig. 3. Simplified equivalent circuit

2) Energy Buffer: The harvester is designed for supercaps with a maximum rated voltage of $V_{max} = 2.7$ V. Results from the literature [1], [7] show that supercaps with 25 to 100 F give a good trade-off between size, capacity, and price; e.g., a 50 F supercap can operate an Iris node at a 1% radio duty cycle for more than two days. The supercap voltage and thus state-of-charge can be read by the sensor node. To protect the supercap from overcharging, the harvester automatically disconnects the solar cell if the supercap voltage exceeds V_{max}. It is possible to disconnect the solar cell manually via the control line S_h, which is connected to an I/O-pin of the micro processor.

3) Switching Regulator: A Texas Instruments TPS 61220 switching regulator [12] supplies the sensor node with a constant voltage of $V_n = 2.7$ V. Its efficiency η ranges from 75% to 95% and it has a cut-off voltage of $V_{cut} = 0.5$ V for our platform. Figure 2 reveals that η only depends on the input voltage but is almost independent of the output current.

B. Equivalent Circuit System Model

1) Simplified Equivalent Circuit: The simplified circuit of our harvester is displayed in Fig. 3. The current $I_h \geq 0$ (the *harvest*) is produced by the solar cell, and the current $I_r \geq 0$ is consumed by the regulator to supply the sensor node with $I_n > 0$ (the *load*) at the constant output voltage V_n and with a conversion efficiency η. The current I_c flows into the supercap with capacity C. If I_c is positive, harvest exceeds consumption and the supercap is charged; otherwise, the supercap acts as source and discharges to supply the sensor node. V_c is the voltage of the supercap. Note that due to overcharging protection, V_c cannot exceed V_{max} and that the regulator will fail, if V_c underruns V_{cut}.

2) Energy-Flow Model: The circuit in Fig. 3 yields the mathematical model

$$I_\mathrm{h} - I_\mathrm{r} = I_\mathrm{c} \quad \text{with} \quad I_\mathrm{r} = \frac{I_\mathrm{n} \cdot V_\mathrm{n}}{\eta \cdot V_\mathrm{c}}\,, \quad I_\mathrm{c} = C \cdot \dot{V}_\mathrm{c}\,. \tag{1}$$

Here, the supercap is modeled as an ideal capacitor, since early results [7], [13] promise that leakage and reorganization effects can be neglected. The regulator efficiency η can be modeled as a constant value or as a function of V_c. We will discuss this issue and its implications in the following.

IV. State-of-Charge Assessment

We derive models for residual energy assessment of supercaps that are suitable for application on low-power and resource-constrained devices. First, we model the charging behavior of supercaps. Second, we describe the voltage course V_c of a pre-charged supercap for a known load I_n.

A. Charging Behavior and Charging Time Estimation

The remaining time until reaching a certain state-of-charge is often needed for scheduling decisions or load adaptations. For that purpose, we model the charging behavior of a supercap for $I_\mathrm{h} \gg I_\mathrm{r}$, giving a lower bound on charging time if this condition is not satisfied. From Sect. III-B2, we deduce

$$I_\mathrm{h} = C \cdot \dot{V}_\mathrm{c}\,. \tag{2}$$

For a starting voltage V_0 at time t_0, (2) can be utilized to either predict the supercap voltage V_c at time $t_0 + \Delta t$ or the expected time Δt until charging to a given voltage V_t has completed. W.l.o.g. we assume $t_0 = 0$ in the following and hence obtain

$$\int_0^{\Delta t} I_\mathrm{h}(t) = C \cdot \int_{V_0}^{V_t} \mathrm{d}V_\mathrm{c}\,. \tag{3}$$

The temporal course of I_h can be replaced by using its (expected) average value $\hat{I}_\mathrm{h}$, yielding

$$V_t = V_0 + \frac{\hat{I}_\mathrm{h}}{C} \cdot \Delta t \quad \Leftrightarrow \quad \Delta t = (V_t - V_0) \cdot \frac{C}{\hat{I}_\mathrm{h}}\,. \tag{4}$$

B. Voltage Course under Load and Lifetime Prediction

We analyze the temporal behavior of the supercap voltage V_c in a situation in which there is no energy intake ($I_\mathrm{h} = 0$), so that the supercap only supplies the sensor node and is being discharged exclusively. This model can be applied to perform pessimistic lifetime estimation, i.e., if energy intake is expected in the future but its course is uncertain or unknown. We neglect self-discharge and reorganization effects and assume $\eta = \mathrm{const.}$. From (1) in Sect. III-B2, we obtain

$$-\frac{V_\mathrm{n} \cdot I_\mathrm{n}}{\eta \cdot V_\mathrm{c}} = C \cdot \dot{V}_\mathrm{c}\,. \tag{5}$$

For a starting voltage V_0 at time t_0, (5) can be utilized to either predict the supercap voltage V_c at time $t_0 + \Delta t$ or the expected time Δt until reaching a given voltage V_t. W.l.o.g. we assume $t_0 = 0$ in the following and hence obtain

$$-V_\mathrm{n} \cdot \int_0^{\Delta t} I_\mathrm{n}(t)\,\mathrm{d}t = \eta C \cdot \int_{V_0}^{V_t} V_\mathrm{c}\,\mathrm{d}V_\mathrm{c}\,. \tag{6}$$

TABLE I
Evaluation node setup

node	nominal C	harvesting source	I_h
A	50 F	solar cell / lamp	8.7 ± 2.8mA
B	50 F	solar cell / lamp	n.a.
C	50 F	const. current source	15.0 mA
D	25 F	solar cell / lamp	7.0 ± 0.8mA
E	25 F	solar cell / lamp	6.5 ± 0.8mA

In this equation, the actual course of I_n does not have to be known, since we can replace the integral by using the (expected) average consumption

$$\hat{I}_\mathrm{n} = \frac{1}{\Delta t} \cdot \int_0^{\Delta t} I_\mathrm{n}(t)\,\mathrm{d}t\,. \tag{7}$$

Finally, (6) can be solved to obtain the future voltage V_t or the expected lifetime Δt for a target voltage V_t:

$$V_t = \sqrt{V_0^2 - \frac{2V_\mathrm{n}\hat{I}_\mathrm{n}\Delta t}{\eta C}} \quad \Leftrightarrow \quad \Delta t = \left(V_0^2 - V_t^2\right) \frac{\eta C}{2V_\mathrm{n}\hat{I}_\mathrm{n}}\,. \tag{8}$$

These equations can be easily used for state-of-charge determination. More importantly, they can be employed to determine the maximum supported, uniform load $\hat{I}_\mathrm{n}$ without predicting the future energy intake. It is possible to use this approach for a basic load adaptation scheme.

However, any application of these equations relies on knowledge about the actual capacity C and regulator efficiency η. Regulator efficiency depends on the input voltage, which is not constant in our case (cf. Sect. III-A3). The previous equations assume a constant efficiency for the sake of model simplicity. A relaxation of this constraint can be achieved by describing η as a piece-wise constant function of V_c. Calculation of V_t or Δt, respectively, can then be realized through an iteration process using (8). This procedure increases computation complexity and scales with the number of η steps. Moreover, a precise and generic—i.e., node-independent—function for η must be known.

V. Evaluation Methodology

Before presenting results in Sect. VI, we explain the methodology, evaluation setup, parameter choice, and metrics.

A. Setup and Parameters

We deployed five Iris sensor nodes powered by our harvester with supercaps with nominal capacities of 25 and 50 F. A desktop light was used to power the solar cells to achieve realistic circuit behavior. The nodes were placed in a frequently used laboratory resulting in node and lamp movements, while sunlight broke through the windows in the afternoons. This resulted in (slightly) changing lighting conditions. The harvester of node C was connected to a constant current source instead to investigate charging in the case of $I_\mathrm{h} = \mathrm{const.}$ A summary of the setup is displayed in Table I.

All nodes ran charge-discharge cycles for the set of parameters shown in Table II, which were picked to resemble common

TABLE II
EVALUATION PARAMETERS

param.	unit	charging	discharging
θ	%	0.2	0.5, 1, 5, 10, 20
V_0	V	1.0	1.4, 1.8, 2.2, 2.6
V_t	V	1.4, 1.8, 2.2, 2.6	1.0
S_h		false	true

sensor node operation and to evaluate the influence of charging target voltage. The harvesting current I_h was measured every 5 s, and an average was computed every30 s—no I_h-readings are available for node B due to sensor failure. All other sensors (cf. Sect. III-A) were read with a period of 30 s. The set of readings plus a timestamp were transmitted to a base station. We simulated radio duty-cycling MAC protocols by switching off the radio after successful packet transmission with a delay corresponding to the current duty cycle θ. For each value of θ we ran one discharging cycle (with disconnected solar cell, cf. Sect. III-A1) for different voltage ranges. For charging the lowest duty cycle was always used, so that the node's consumption could be neglected (cf. Sect. IV-A).

B. Evaluation Methodology and Metrics

For each discharging and charging trace, we derived empirical values of C by minimizing the root-mean-square-error (RMSE) using (4) and (8), respectively. We also calculated C values for 0.1 V-intervals of each trace. We chose involved parameter values as in Sect. III-A and used a constant efficiency of $\eta = 87.5\%$. An evaluation using a step-function of η at 0.1 V granularity is omitted due to space constraints. The values of I_h and I_n were derived from the sensor node readings and using the nodes' measured average consumption profile. This particularly implies that the results show a picture from the perspective of a sensor node with imprecise consumption knowledge, temperature dependency, and error-afflicted sensor readings. This allows us to answer the question of whether simple models are sufficient for sensor nodes.

VI. EVALUATION

In the following, we present the evaluation of our experiment and analyze the accuracy of our models.

A. Charging Behavior

All charging traces of our experiment exhibit an almost linear voltage increase and thus support (4). Figure 4 shows an example trace. However, charging slows down for large values of V_c for two reasons. Firstly, I_h decreases slightly with increasing V_c (except for node C), since the power-point of the solar cell is changed. Secondly, reorganization effects have a more notable influence for larger values of V_c [7], [8].

A detailed study of C w.r.t. V_c is displayed in Fig. 5. Both plots show similar average empirical C and reveal that variation is also low. We can hence conclude that supercap charging is highly predictable in low-power sensor networks using (4), if I_h is known. Only for V_c approaching V_max

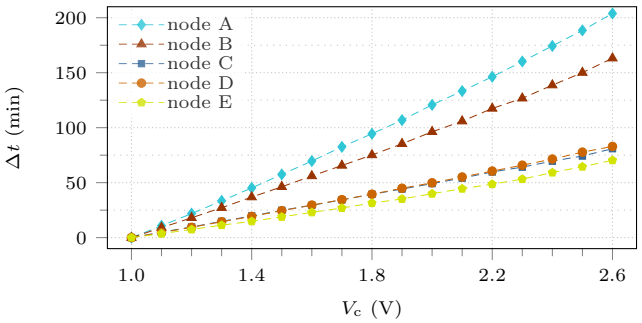

Fig. 4. Charging traces supporting near-linear time-voltage dependency

(Fig. 5a), the empirical C increases, i.e., charging slows down. The model will hence produce too large voltage projections or too small charging time estimates, respectively.

The distribution of the average C for the individual charging procedures is shown in Fig. 6. Variation is within 0.5 F, and capacity is slightly larger when charging to a higher V_c. The figure supports that charging time estimation with a single, empirically determined C is feasible and sufficiently accurate, particularly if sensor readings or estimates of I_h are error-afflicted or uncertain due to changing harvesting conditions. Using nominal capacities would introduce large errors.

B. Voltage Course under Load and Lifetime Prediction

The voltage course under load generally exhibits the shape expected from (8). Figure 7 shows the actual remaining lifetime for two different θ and compares the traces with ideal projections of our model. Deviations from the model are particularly notable at high voltages V_c. This supports previous findings about reorganization effects at high voltages. Whether the charging duration and voltage difference also have an influence is not clear and requires further investigation. However, since lifetime overestimation does not pose a severe depletion hazard at high values of V_c (corresponding to high energy reserves), the model error is tolerable in a practical sensor node deployment.

Under load, empirical capacities show slightly larger fluctuation than for charging and the dependency on V_c is inverse. This is indicated by Fig. 8. The mean capacity is smaller than for charging in most cases. This offset may be caused by error-afflicted consumption and harvest readings. Particularly for low duty cycles, small absolute errors in consumption tracking may lead to significant errors in state-of-charge assessment and lifetime prediction, which supports our case for simple models: In practical application, models need not be more accurate than their input values. Figure 9 further stresses this point: Here, marks in the plot indicating larger empirical capacity stem from the runs with lower θ.

C. Model Errors

We analyzed the RMSE error of three variants of our model; the results are displayed in Fig. 10. For all nodes, we calculated the errors between our model and the recorded load traces for three approaches. First, we used optimized values

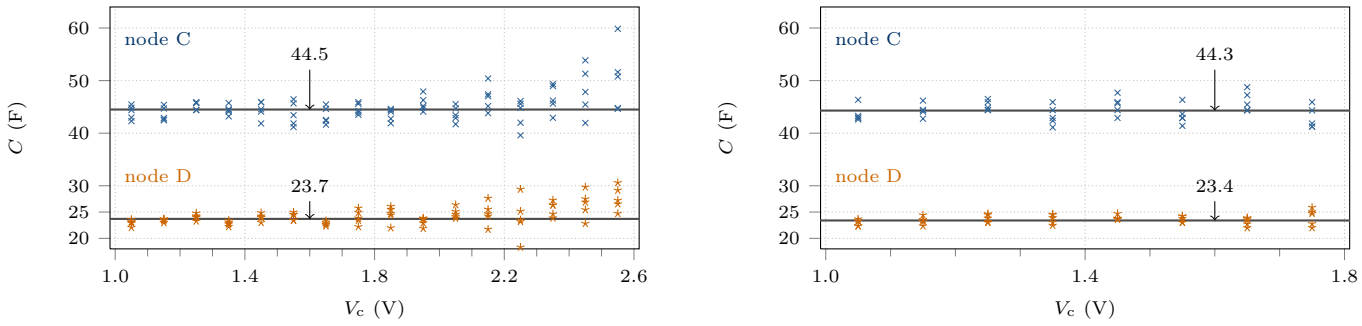

(a) $V_t = 2.6\,\mathrm{V}$ (b) $V_t = 1.8\,\mathrm{V}$

Fig. 5. Empirical, unbiased capacity estimates at intermediate voltages of nodes C and D during charging. Solid lines indicate average capacity, cf. Fig. 6

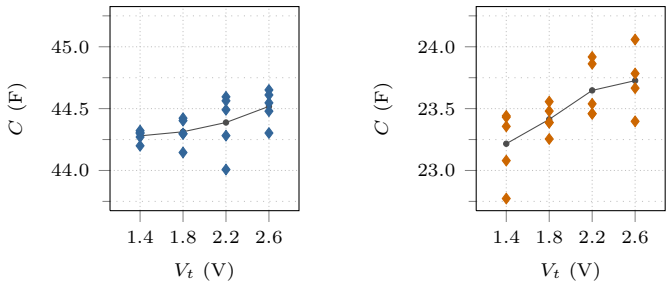

(a) node C (b) node D

Fig. 6. Average empirical capacity for charging to different V_t. The gray line represents the mean value of charging traces with same V_t

of C for each individual trace to identify the smallest possible model error. It shows that the relative RMSE never exceeds 2% in this case. Second, we used a single value of C that was obtained by averaging the empirical capacities at 2.2 V. The relative RMSE is always below 5% with a median of 2% in the worst case. Third, we used the nominal capacity, printed on the supercaps, giving errors of up to 22% and medians of 3 to 13%. The distribution of errors varies notably among supercaps due to age, usage, and manufacturing deviation.

These results have the following impact. Firstly, despite the simplicity of our model, it allows for producing low-error of state-of-charge assessment in most cases. Secondly, using a static, online-estimated capacity value increases errors but keeps them within the range of common sensor node consumption variance [14]. This approach is hence feasible. Thirdly, using the nominal capacity printed on the supercaps results in large, intolerable errors. Therefore, consumption deviation among nodes caused by hardware variation is merely insignificant compared to errors in capacity estimation.

Our evaluation shows that the proposed models work in the field. Errors may be as large as 5%, but this number is small when considering that sensor nodes have (slightly) different consumption, yet only the mean consumption among all nodes is used for evaluation, and although a constant regulator efficiency is employed. Improved results are possible at the cost of hardly feasible per-node consumption configuration. Despite different charging currents and duration, target voltage, and capacity, all discharging traces exhibit an almost equal shape that show high correlation with the modeled behavior.

VII. Conclusion

We have presented simple models for state-of-charge assessment on real sensor node hardware. Various charging and discharging traces for common sensor node duty cycles certify small model errors. More importantly, the errors using a real-world compatible implementation with a static, online-estimated capacity are below 5% in all cases and below 2% on average. The proposed method for state-of-charge estimation is hence sufficiently accurate for application on sensor nodes, particularly w.r.t. consumption uncertainties due to hardware variation and error-afflicted sensor readings. These observations hold for a wide range of hardware, since most sensor nodes and low-power switching regulators and solar cells have similar characteristics to the ones used in this paper.

Our results emphasize the need for online capacity calibration. Practical approaches have been addressed in [13]. However, additional points must be considered, e.g., calibration should not be performed directly after a charging procedure, since capacity estimates tend to be too small in this case. Picking the right supercap voltage range for calibration is also important to obtain a representative value of C. Further investigation on this matter is scheduled for the near future.

References

[1] X. Jiang, J. Polastre, and D. Culler, "Perpetual Environmentally Powered Sensor Networks," in *Proc. Intl. Symp. on Information Processing in Sensor Networks*, ser. IPSN, 2005.

[2] F. Simjee and P. H. Chou, "Everlast: Long-Life, Supercapacitor-Operated Wireless Sensor Node," in *Proc. Intl. Symp. on Low Power Electronics and Design*, ser. ISLPED, 2006.

[3] V. Kyriatzis, N. S. Samaras, P. Stavroulakis, H. Takruri-Rizk, and S. Tzortzios, "Enviromote: A New Solar-Harvesting Platform Prototype for Wireless Sensor Networks," in *Proc. Intl. Symp. on Personal, Indoor and Mobile Radio Communications*, ser. PIMRC, 2007.

[4] C. Renner and V. Turau, "Policies for Predictive Energy Management with Supercapacitors," in *Proc. 8th Intl. Wksp. on Sensor Networks and Systems for Pervasive Computing*, ser. PerSeNS, 2012.

[5] C. Moser, L. Thiele, D. Brunelli, and L. Benini, "Adaptive Power Management for Environmentally Powered Systems," *IEEE Trans. on Computers (TC)*, vol. 59, no. 4, 2010.

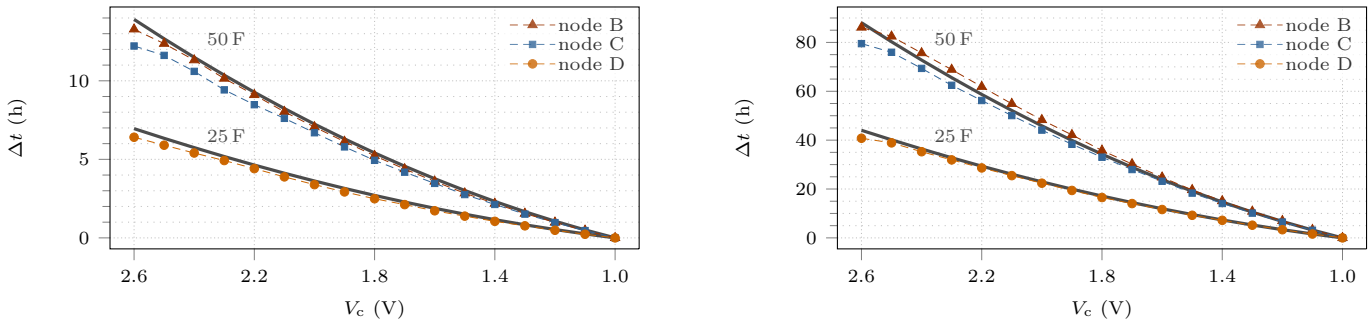

(a) $\theta = 5\%$ (b) $\theta = 0.5\%$

Fig. 7. Remaining lifetime until reaching 1.0 V at intermediate voltages V_c for two common duty cycles. Charging was immediately stopped at 2.6 V. Solid gray curves indicate modeled lifetime estimates for the nominal capacities of the used supercaps.

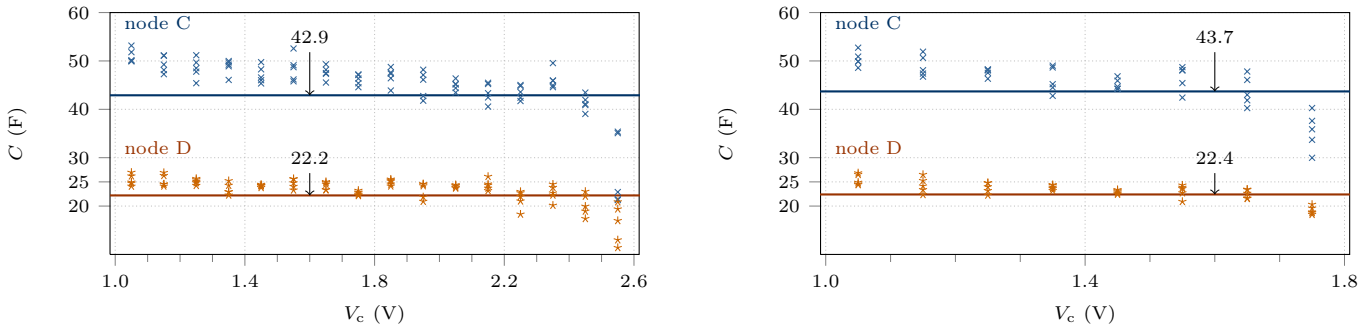

(a) $V_0 = 2.6$ V (b) $V_0 = 1.8$ V

Fig. 8. Scatter plot of empirical capacities versus V_c at 0.1 V granularity for different θ. Solid lines indicate average capacity for the same data basis

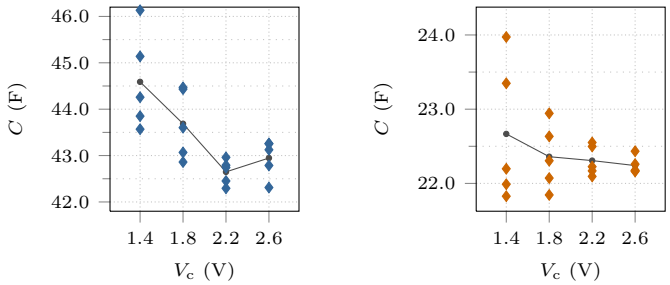

(a) node C (b) node D

Fig. 9. Average empirical capacity under load until for different V_0. The gray line represents the mean value of traces with same V_0

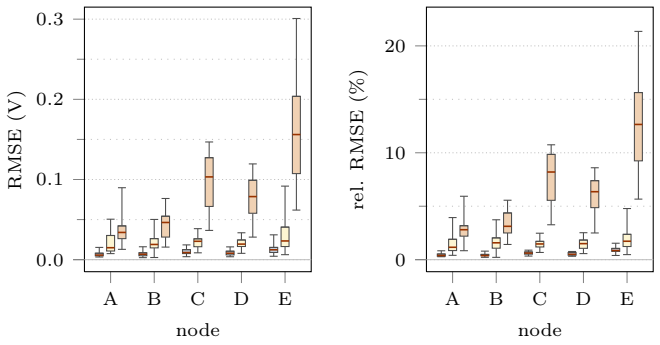

(a) RMSE (b) rel. RMSE

Fig. 10. Discharging model errors using C values optimized for each load curve (blue/left), a single estimated C value at $V_c = 2.2$ V (yellow,center), and the nominal C (orange,right). The boxplots show median, quartiles, and extrema using all discharging curves at a granularity of 30 s

[6] SAMWHA Electric Co., Ltd., *Green Cap Datasheet*. [Online]. Available: http://www.samwha.co.kr/SW_Catalogue/ecatalog.asp?Dir=60

[7] C. Renner, J. Jessen, and V. Turau, "Lifetime Prediction for Supercapacitor-powered Wireless Sensor Nodes," in *Fachgespräch Sensornetze (expert talk on sensor networks)*, ser. FGSN, 2009.

[8] A. Weddell, G. Merrett, T. Kazmierski, and B. Al-Hashimi, "Accurate Supercapacitor Modeling for Energy-Harvesting Wireless Sensor Nodes," *Trans. on Circuits and Systems II: Express Briefs*, vol. 59, 2011.

[9] P. Dutta, J. Hui, J. Jeong, S. Kim, C. Sharp, J. Taneja, G. Tolle, K. Whitehouse, and D. Culler, "Trio: Enabling Sustainable and Scalable Outdoor Wireless Sensor Network Deployments," in *Proc. 5th Intl. Conf. on Information Processing in Sensor Networks*, ser. IPSN, 2006.

[10] P. Barrade and A. Rufer, "Current Capability and Power Density of Supercapacitors: Considerations on Energy Efficiency," in *Proc. 10th Europ. Conf. on Power Electronics and Applications*, ser. EPE, 2003.

[11] T. Zhu, Z. Zhong, Y. Gu, T. He, and Z. Zhang, "Leakage-Aware Energy Synchronization for Wireless Sensor Networks," in *Proc. 7th Intl. Conf. on Mobile Systems, Applications and Services*, ser. MobiSys, 2009.

[12] Texas Instruments, *Datasheet TPS 61220*, 2009. [Online]. Available: http://focus.ti.com/lit/ds/symlink/tps61220.pdf

[13] C. Renner and V. Turau, "CapLibrate: Self-Calibration of an Energy Harvesting Power Supply with Supercapacitors," in *Intl. Conf. on Architecture of Computing Systems*, ser. ARCS, 2010.

[14] C. Haas, V. Stöhr, and J. Wilke, "Realistic Simulation of Energy Consumption in Wireless Sensor Networks," in *Proc. 9th European Conf. on Wireless Sensor Networks*, ser. EWSN, 2012.